Enhanced Ultrasound Localization Microscopy with Spatio-Temporal Deep Learning

V. Pustovalov, **D. H. Pham**, **D. Kouamé**

MINDS Team, IRIT, Université Toulouse III Paul Sabatier, France.

October 2024

Université Fédérale
Toulouse Midi-Pyrénées

Outline

Introduction

Clinical Context

- **Non-invasive stroke diagnosis:**
  Avoid MRI and CT-scan constraints.

Figure 1: CT-scan with hemorrhage in the left thalamus.

- **Surgical management of cerebral gliomas:**
  Infiltrating gliomas have no clear boundary with healthy tissue.
  May be located close to or within "functional" brain areas

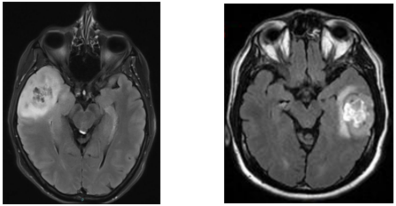

Figure 2: Diffuse high-grade gliomas.

Experimental procedure

- Contrast enhanced ultrasound:
  Preparation and installation
  Microbubble injection

- Ultrafast Ultrasound Imaging:
  High pulse repetition frequency
  Beamforming (DAS)

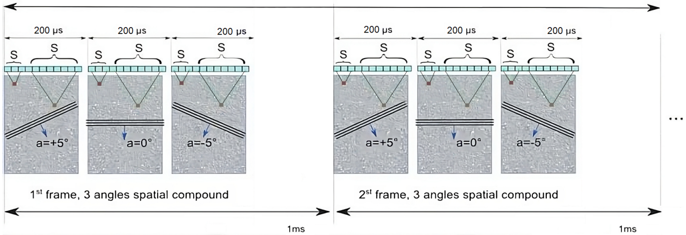

Figure 3: An US acquisition at a compounded frame rate of 1,000 Hz with 3 tilted plane waves [-5°,0°, +5°].

ULM Pipeline

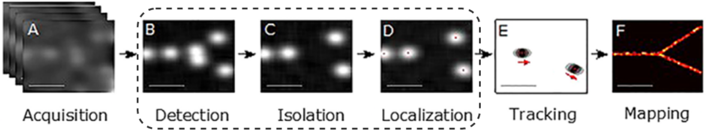

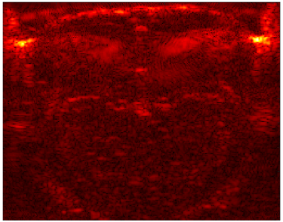

Bmode IQ

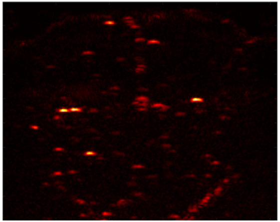

Clutter Filtered

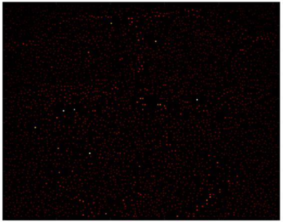

Regional Max

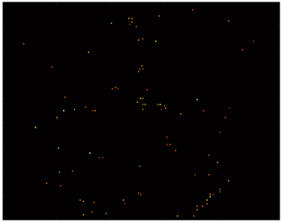

Amp Filtering

Proposed approach

ULM CNNs limitations

- **Scarcity of labeled In Vivo data.**
- **Use of high-resolution grid.**

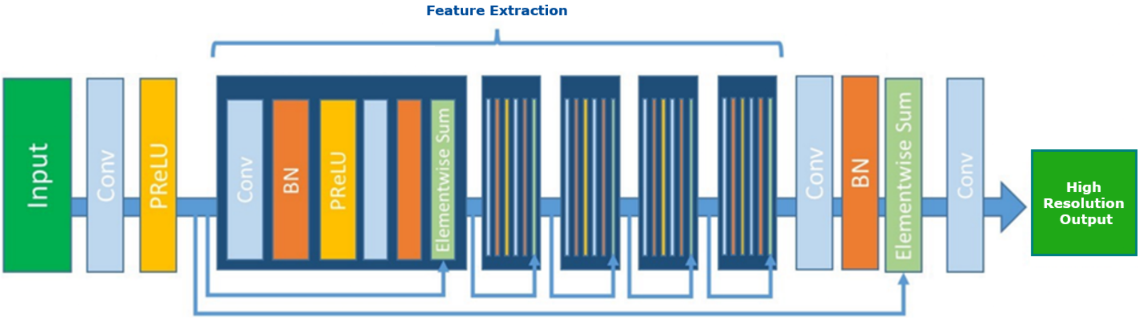

US simulation from MRI

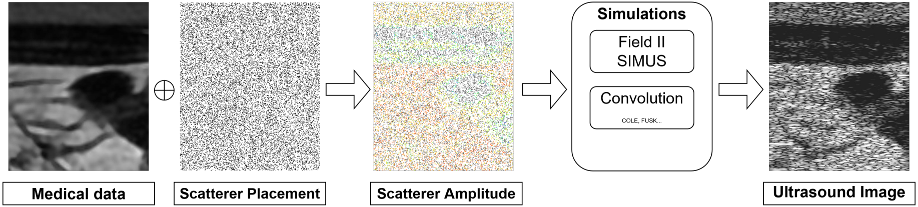

Figure 4: Standard scatterer based ultrasound simulation.

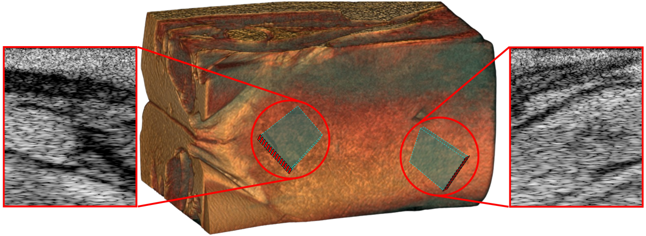

Figure 5: Simulated US images using MRI volume slices.

CAM simulation data

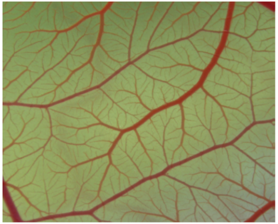

CAM image

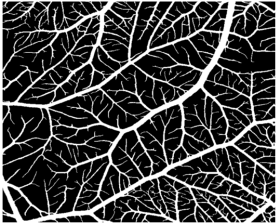

Segmented Vessels

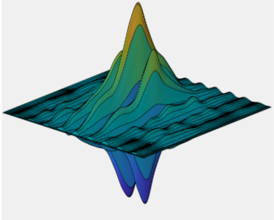

Extracted PSF

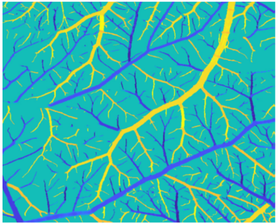

X displacement map

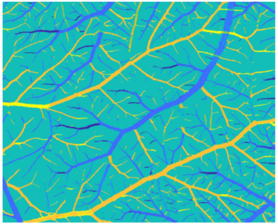

Y displacement map

Bmode US frame

Proposed Method

- Output Representation:

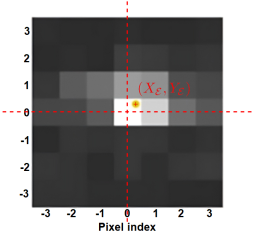

- Network Loss function:

$$Loss = L_{pos} + L_{loc} \tag{1}$$

$$L_{pos} = \left\| H \circledast Pos - H \circledast \hat{Pos} \right\|_F^2 \tag{2}$$

$$L_{loc} = \frac{1}{2} \left\| X_{\mathcal{E}} - \hat{X_{\mathcal{E}}} \right\|_F^2 + \frac{1}{2} \left\| Y_{\mathcal{E}} - \hat{Y_{\mathcal{E}}} \right\|_F^2 \tag{3}$$

3DML-ResNet Architecture

- Proposed 3DML-ResNet:

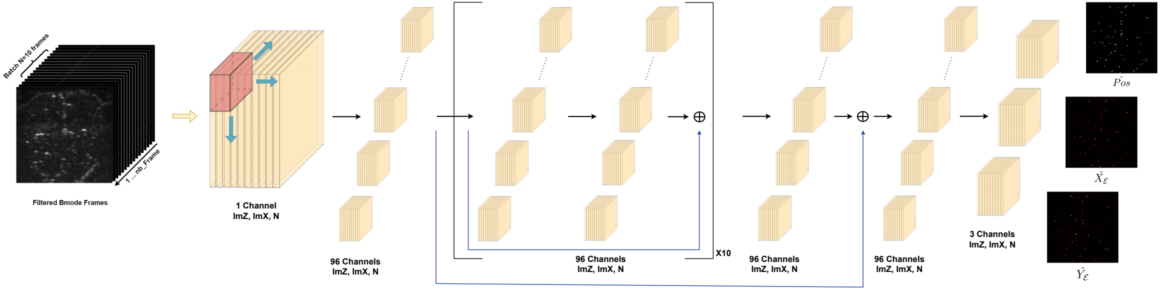

Numerical Results

CAM data Rendering

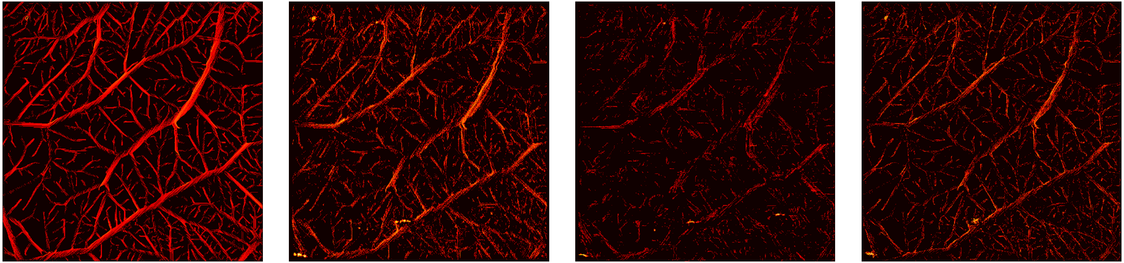

(a) Ground Truth (b) RS ULM [Hei+22] (c) mSPCN [Liu+20] (d) 3DML-ResNet

In Silico PALA Results

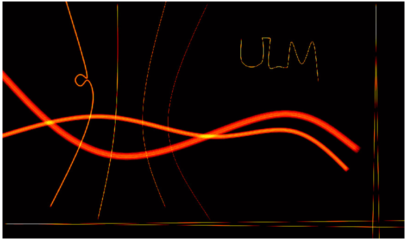

(a) Ground Truth

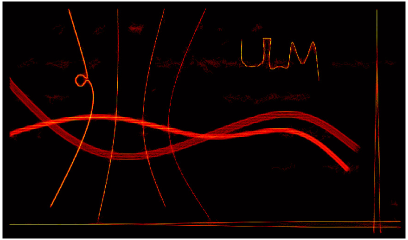

(b) RS ULM [Hei+22]

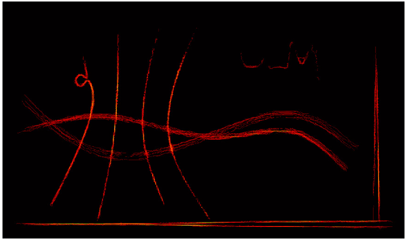

(c) mSPCN [Liu+20]

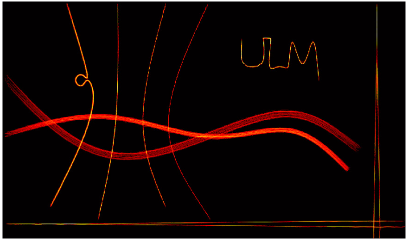

(d) 3DML-ResNet

Metrics

- **PALA In Silico [Hei+22] metrics comparison:**

	RS ULM	mSPCN	3DML-ResNet (Ours)
SSIM [%]	84.37	84.14	**91.40**
RMSE	7.043	9.440	**6.616**
Jaccard Index [%]	24.15	20.54	**47.53**

- **CAM Data [Che+23] metrics comparison:**

	RS ULM	mSPCN	3DML-ResNet (Ours)
SSIM [%]	40.34	42.02	**54.43**
RMSE	2.009	2.892	**1.764**
Jaccard Index [%]	8.13	5.80	**14.29**

In Vivo Rat Brain PALA Results

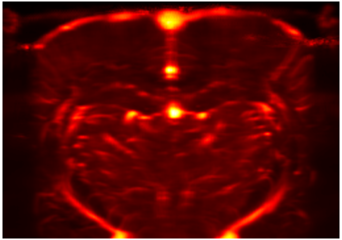

(a) Power Doppler

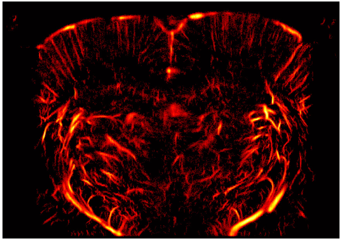

(b) RS ULM [Hei+22]

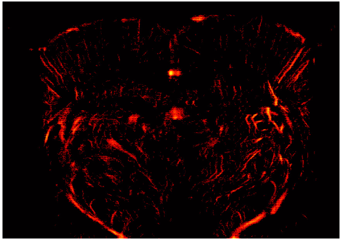

(c) mSPCN [Liu+20]

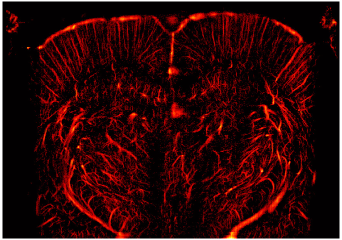

(d) 3DML-ResNet

Thank you!

Questions ?

References

[Hei+22] B. Heiles et al. "Performance benchmarking of microbubble-localization algorithms for ultrasound localization microscopy". In: *Nat. Biomed. Eng.* 6 (2022), pp. 605–616. DOI: 10.1038/s41551-021-00824-8.

[Liu+20] Xin Liu et al. "Deep Learning for Ultrasound Localization Microscopy". In: *IEEE TMI* 39.10 (2020), pp. 3064–3078. DOI: 10.1109/TMI.2020.2986781.

[Che+23] Xi Chen et al. "Localization Free Super-Resolution Microbubble Velocimetry Using a Long Short-Term Memory Neural Network". In: *IEEE TMI* 42.8 (2023), pp. 2374–2385. DOI: 10.1109/TMI.2023.3251197.